Comparison of Hardness and Residual Stresses in Multiline Laser Surface Hardening and Induction Hardening

Philipp Schüßler[1,*1], Niki Nouri[1,*1], Stefan Dietrich[1] and Volker Schulze[1]

[1] *Institute for Applied Materials – Materials Science and Engineering (IAM-WK) / Karlsruhe Institute of Technology (KIT), 76131 Karlsruhe, Germany*

This study investigates the differences between induction hardening and multiline laser surface hardening processes on AISI 4140 quenched and tempered steel in order to guide the process selection based on the resulting material properties. The microstructures and hardness profiles resulting from the two processes were analyzed and different characteristics were observed. Induction hardening demonstrates rapid processing and uniform hardening, but with negative aspects such as edge effects and depth limitations. In contrast, multiline laser surface hardening offers adaptability to different geometries. Due to tempering effects, a layered microstructure was noted with a lower hardness for previously processed areas. This study sheds light on the strengths and limitations of these two surface hardening techniques, providing insight into the selection of optimal processes for enhancing material properties.

Keywords: *induction hardening, multiline laser surface hardening, microstructure, hardness*

1. Introduction

Structural components manufactured from quenched and tempered steels, such as AISI 4140, frequently withstand significant mechanical loads during their operational lifespan. Since failures often occur on the surface of components, surface hardening processes are used to improve the load-bearing capacity in those areas [1)]. Laser surface hardening and induction hardening are two of the most commonly used thermal surface hardening methods. They are often chosen based on their respective advantages and disadvantages in terms of achievable geometries, set-up flexibility, processing times and cost. Laser surface hardening employs a laser to heat the surface of the parts locally, with the bulk of the material serving as a heatsink, cooling the heated surface through conduction. Due to the high flexibility of positioning and moving the laser with laser scanners and/or robots and the variation of the spot size the process can be easily adapted to a wide range of parts. Several modes of laser surface hardening, such as spot hardening [2)], single line hardening [3–5)], and multiline hardening [6,7)] have been extensively researched, but lack in direct comparisons with other processes. In contrast to laser surface hardening, the induction hardening process utilizes a copper inductor to rapidly heat the work piece by inducing eddy currents near the surface. Subsequently, the work piece is cooled to room temperature by a water shower after heating. Induction hardening has several advantages. These include short process times, high process efficiency and a uniformly hardened surface [8)]. Induction hardening is widely used for rotationally symmetric work pieces, such as gears and shafts, as identified in literature [1,9,10)]. This study aims to provide key insights into both laser surface hardening and induction hardening processes when compared for the quench and tempering steel AISI4140. By examining the microstructure and hardness of these two processes on the same demonstrator geometry, this study uncovers their strengths and limitations. This enables the selection of the optimal process type for the surface hardening of similar components.

2. Experiment

2.1 Material

The experiments were carried out with the low alloyed steel AISI 4140 (German grade 42CrMo4) in a quenched and tempered state. The initial hardness of the quenched and tempered microstructure was measured to 360 $HV_{0.1}$. The chemical composition in wt.% is shown in Table 1. A cylindrical demonstrator with a diameter of 50 mm and a thickness of 5 mm was used.

Table 1 Chemical composition of the used batch of AISI 4140 in wt.%.

C	Si	Mn	Cr	Mo	Fe.
0.42	0.22	0.69	0.94	0.16	Bal.

2.2 Induction hardening experiments

For the induction hardening process, a single-shot approach was employed on an industrial-grade induction hardening machine (Fiand KHM 750, Fiand Automatisierungstechnik GmbH, Germany) using a dual-frequency converter (IDEA SMS850, IDEA GmbH, Germany). The generator of the hardening machine allows a simultaneous dual frequency inductive heat treatment with a maximum power output of 850 kW and frequency bands of 10 – 30 kHz for the medium frequency range (MF) and 150 – 450 kHz for the high frequency range (HF) mode. In order to achieve the same depth of hardening as with the laser surface hardening process, only the HF mode was used. Since the inductor's geometry significantly influences heat generation in the work piece, it was specifically optimized for this demonstrator work piece [1)]. The optimized process parameters were determined to be a heating time of 75 ms and a power of 72 kW (16 % of the 450 kW) in the HF mode. The inductance of the inductor resulted in a resonance frequency of 175 kHz for all experiments. In order to achieve the desired cooling rates, the samples were quenched to room temperature by a spray head with a water-polymer-mixture spray. Temperature data was logged by a thermocouple (Type K) welded on the outer diameter of the demonstrator piece.

---

*1 Graduate Student, Karlsruhe Institute of Technology (KIT)

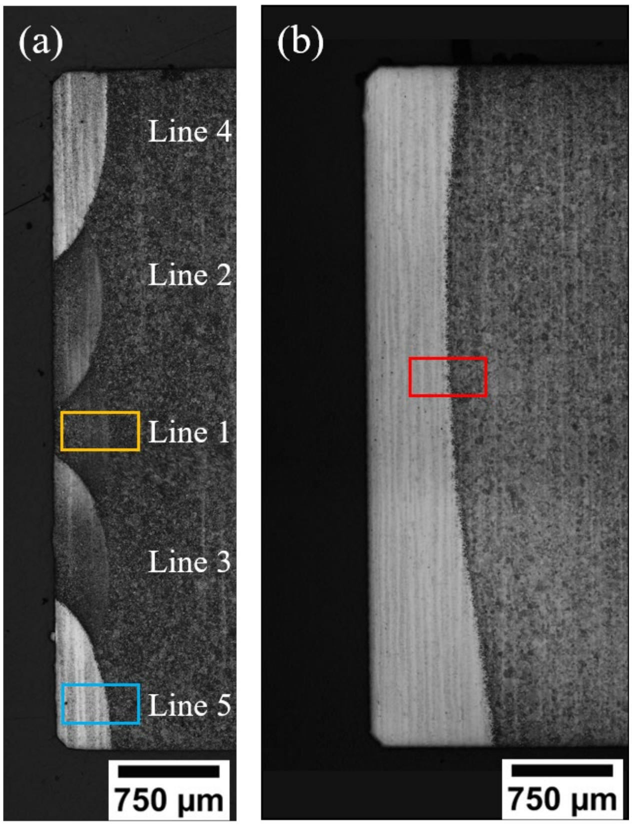

Figure 1 Microstructure of the polished and etched radial cross section. Visualizing the overview of the hardened zone for (a) multiline laser surface hardening and (b) induction hardening.

2.3 Laser hardening experiments

For the laser hardening experiments, a single line hardening process was not possible due to the limitation of the used laser optics. A multiline laser surface hardening process was used in order to harden the outer diameter of the demonstrator piece. A robotic arm was used for axial positioning in combination with a stationary single-mode fiber laser (SPI Lasers UK Ltd., United Kingdom). The laser had a spot diameter of 1 mm, a wavelength of 1080 nm, and a maximum power of 500 W. Five lines with different parameter combinations were needed in order to achieve a continuous hardening depth of about 400 µm. All lines were processed with a scan speed of 5 mm/s. A laser power of 160 W was used for the center line (line 1), 140 W for the two adjacent lines (line 2 and line 3) and 120 W for the outer most lines (line 4 and line 5).

2.4 Metallographic characterization

After the surface heat treatment, all samples were cut in axial direction. The resulting longitudinal cross section was embedded, ground and polished up to 1 µm. The subsequent hardness measurements were done with a Vickers hardness tester (Qness Q30A+, ATM Qness GmbH, Germany) and a testing load of 10 N. In order to visualize the local hardness differences complete scans including the hardened zone, heat affected zone and the base material were conducted. The minimum distance between two measured points was 50 µm. For the investigation of the microstructure, the samples were polished up to 0.04 µm and subsequently etched with 1 % nital (1 % nitric acid with 99 % ethanol) etchant for 3 s.

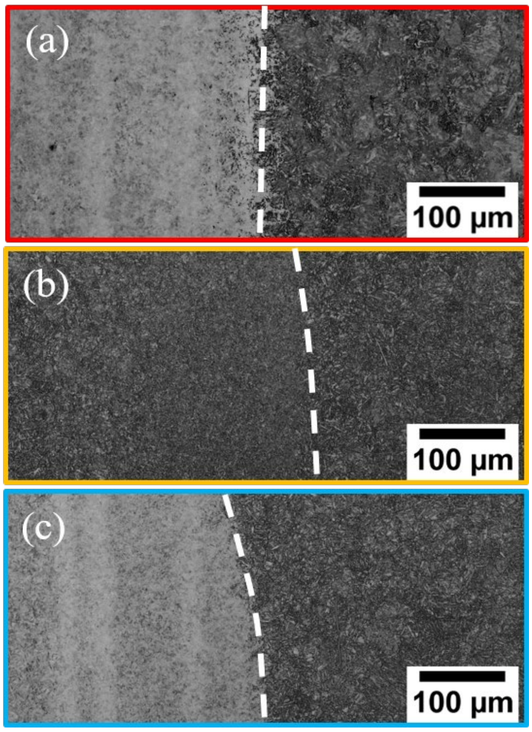

Figure 2 Microstructure of the polished and etched radial cross section. Visualizing (a) the transition zone for the induction hardening, (b) the transition zone for line 1 of the multiline laser surface hardening, (c) the transition zone for line 5 of the multiline laser surface hardening.

3. Results

3.1 Microstructure

The microstructure after hardening is visualized in Fig. 1 and Fig. 2 for induction hardening and the multiline laser surface hardening process. The induction hardening process leads to a homogeneous martensitic microstructure at the surface, with a hardening depth of about 500 µm in the center of the hardened zone and about 700 µm closer to the edges (Fig. 1 (b)). A sharp transition from the hardened zone to the tempered base material is noted. The base material consists of highly tempered martensite with a visible lath structure. The multiline laser surface hardening process leads to a layered microstructure with all single lines of the process clearly visible after etching (Fig. 1 (a)). Due to the hardening sequence, a highly tempered martensitic microstructure is visible in the center area, a graded microstructure in the areas of line 2 and 3 and a fully martensitic microstructure on the outside areas (Fig. 2).

3.2 Hardness

In order to characterize the differences shown in the microstructure analysis (Sec. 3.1), the hardness after both processes was characterized by a full size hardness mapping of the hardened zone and the base material (Fig. 3). These results show the expected correlation between the microstructure and hardness measurements. While the induction hardening process leads to a homogeneous hardness in the process zone, the multiline laser surface hardening process shows a layered hardness profile with significantly lower hardness in the center of the process zone. These results are in line with the microstructure shown in Sec. 3.1. The laser surface hardening process results in a

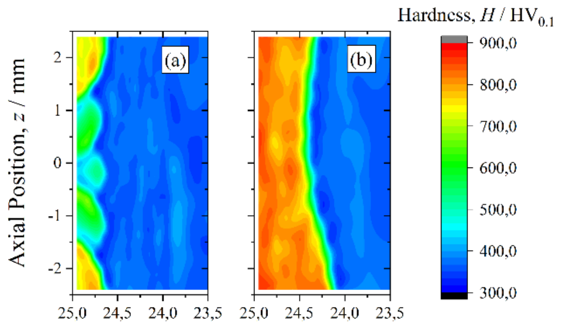

Figure 3 Visualization of the measured hardness map for (a) the multiline laser surface hardening process and (b) the induction hardening process.

shallower hardening depth of about 400 µm with a maximum hardness of 790 $HV_{0.1}$. In contrary, the induction hardening leads to a hardening depth of about 500 µm in the center of the process zone with a maximum hardness of about 860 $HV_{0.1}$. A narrow tempered zone of about 200 µm thickness is noted for both processes between the hardened zone and the base material, resulting in the global minimum hardness of 340 $HV_{0.1}$, 20 $HV_{0.1}$ lower than the base material.

4. Discussion

While the induction hardening process has many advantages, such as very short process times and high accuracy, the process is limited to simple geometries with an inductor optimized for each geometry. This negative effect can be seen in the microstructure images (see Figure 1) and the corresponding hardness map (see Figure 3) of the cross sections. Even though a simple demonstrator was used, inhomogeneities in the magnetic field density lead to significant edge effects, resulting in higher temperatures and therefore higher hardening depths at the exposed edges of the part. A smaller hardening depth was not possible due to the machine's frequency limitations. A higher frequency would be beneficial in order to reduce the hardening depth. A further reduction in heating time was not possible due to machine control hardware and software limitations. In contrast to induction hardening, multiline laser surface hardening is a very flexible process that can be easily adapted to different geometries. A variation of the spot size could therefore significantly influence the resulting microstructure as well as the hardness profile. The tempering process can explain the differences in surface hardness, as subsequent lines are hardened in close proximity. Since the maximum temperature in these regions stays below the austenitization temperature, this results in tempering of the previously formed martensite. As a result, the maximum hardness in these areas was reduced, but the hardness was still significantly higher when compared to the base material. Consequently, these tempering effects can limit the potential applications, as the inhomogeneous microstructure can introduce a metallurgical notch effect. Furthermore, the significant increase in process time can lead to increased cost when working with bigger parts.

5. Conclusions

In conclusion, the comparative analysis of microstructures and hardness profiles resulting from induction hardening and multiline laser surface hardening processes reveals different characteristics and implications for material properties. The results highlight the potential for tailoring material properties based on process selection. The key highlights of this study are:

(1) Microstructure images and hardness profiles reveal distinctive characteristics of induction hardening and multiline laser surface hardening.
(2) Induction hardening results in a fully hardened zone, while the multiline laser surface hardening produces a layered microstructure.
(3) Induction hardening excels in process times, but exhibits edge effects and depth limitations.
(4) Multiline laser surface hardening offers adaptability but introduces highly tempered zones.

Based on this study, the laser surface hardening process is more suitable for small batch sizes and complex parts requiring a flexible machine setup, while the induction hardening process is favorable for large batch sizes and rationally symmetric parts due to the favorable microstructure and hardness profiles.

Acknowledgments

The authors would like to thank Pierre Lapouge (PIMM Laboratory, Arts et Métiers ParisTech) for providing access and support during for the laser surface hardening experiments.

References

1) F. Mühl, J. Jarms, D. Kaiser, S. Dietrich, and V. Schulze, Materials & Design **195** (2020) pp. 108964.
2) T. Mioković, V. Schulze, O. Vöhringer, and D. Löhe, Acta Materialia **55** (2007) pp. 589–599.
3) P. Schüßler, J. Damon, F. Mühl, S. Dietrich, and V. Schulze, Computational Materials Science **221** (2023) pp. 112079.
4) D. Kiefer, N. Simon, F. Beckmann, F. Wilde, and J. Gibmeier, Optics & Laser Technology **140** (2021) pp. 106964.
5) D. Kiefer, P. Schüßler, F. Mühl, and J. Gibmeier, HTM Journal of Heat Treatment and Materials **74** (2019) pp. 23–35.
6) R. S. Lakhkar, Y. C. Shin, and M. J. M. Krane, Materials Science and Engineering: A **480** (2008) pp. 209–217.
7) F. Cordovilla, Á. García-Beltrán, P. Sancho, J. Domínguez, L. Ruiz-de-Lara, and J. L. Ocaña, Materials & Design **102** (2016) pp. 225–237.
8) M. Schwenk, J. Hoffmeister, and V. Schulze, J. of Materi Eng and Perform **22** (2013) pp. 1861–1870.
9) V. Rudnev, D. Loveless, R. L. Cook, and M. Black, *Handbook of Induction Heating* (CRC Press, Boca Raton, FL, 2002) First edition, Manufacturing Engineering and Materials Processing.
10) D. Kaiser, B. de Graaff, A. M. Jung, S. Dietrich, and V. Schulze, Materials Science and Engineering: A **705** (2017) pp. 114–121.